S-matrix theory of inelastic vibronic ionization of molecules in intense laser fields

A. Requate,[1,2] A. Becker,[1] and F. H. M. Faisal[2]
[1]*Max-Planck-Institut für Physik komplexer Systeme, Nöthnitzer Strasse 38, D-01187 Dresden, Germany*
[2]*Fakultät für Physik, Universität Bielefeld, Postfach 100131, D-33501 Bielefeld, Germany*
(Received 16 November 2005; published 3 March 2006)

Inelastic vibronic ionization (IVI) in the presence of an intense laser field refers to the process of ionization of a target molecule accompanied by vibrational excitation of the residual molecular ion. The recently proposed intense-field many-body *S*-matrix theory of IVI is presented and applied to investigate the distributions of the vibrational states of the residual H_2^+ ion from ionization of H_2 molecule, and the results are compared with the experimental data. The characteristic features of the calculated distributions are found to agree well with those observed. The shift of the IVI distributions toward the lower vibrational states compared to the Frank-Condon distributions, the positions of the maxima of the distributions, as well as the reversal of the maximum from a lower vibrational state to a higher vibrational state (peak-reversal) are analyzed. The results of the "adiabatic nuclei" theory and the "frozen nuclei" approximation are compared to assess the latter. Influences of the choice of the vibrational wave functions on the calculated distributions, the dependence of the distributions on the alignments of the molecular axis with respect to the linear polarization direction of the laser, and the effect of circular polarization of the laser on the IVI distribution are discussed. Possible origins of the remaining discrepancy in the individual heights of the calculated vs. measured yields are pointed out. Finally, an isotopic shift of the IVI distributions toward the higher vibrational states, for the heavier isotopes, is predicted and the corresponding distributions for the two isotopes HD and D_2 are given.

DOI: 10.1103/PhysRevA.73.033406 PACS number(s): 42.50.Hz, 33.20.Wr

I. INTRODUCTION

In recent years there has been much progress in understanding the interactions of molecules with intense laser pulses (for reviews see Refs. [1–4]). A variety of processes, such as single and multiple ionization, harmonic generation, dissociative ionization, or fragmentation have been observed. Of particular interest, in the response of molecules to an external field, are the effects of the extra degrees of freedom, such as alignment, vibration, and rotation of the nuclear frame, which are absent in the case of atoms.

Ionization of molecules with vibrational excitation of the residual molecular ion [referred to here as "inelastic vibronic ionization" (IVI)] in a laser field, is often the precursor of fragmentation of a molecule in the field. The IVI distributions have been at first thought to simply follow the Franck-Condon principle, as in the ionization of molecules by weak synchrotron radiation or fast electron impact. The population in the vibrational states of the molecular ion in that case follows the distribution of the well-known Franck-Condon factors, which are given by the overlap of the vibrational wave functions of the neutral molecule and the molecular ion (e.g., Ref. [5]). But, in a recent experiment [6] it has been found that the relative populations of the vibrational states of H_2^+, arising from the IVI of H_2 molecule in a laser field, are shifted toward the lowest vibrational levels and thus do not follow the assumption of a Franck-Condon (FC) distribution.

Deviations from the FC distributions have been predicted before its observation in static-field calculations [6–8] and subsequently in calculations [9] within the *S*-matrix-*cum*-overlap model. In the former work the fixed nuclei ionization rates were calculated accurately in a static field, and the vibrational transitions were estimated heuristically by taking the matrix element of the "square root of the ionization rates" between the vibrational states. This showed that in strong static fields the variation of the ionization rates with internuclear distance can lead to vibrational distributions of the residual ions that depart significantly from the Franck-Condon distribution. In the *S*-matrix-*cum*-overlap model, on the other hand, the overlap approximation has been assumed, and the transition matrix elements of strong-field ionization of molecules at the equilibrium distance [10] have been simply multiplied with the Franck-Condon overlap factors. The results showed a shift in the population toward lower vibrational levels, which were interpreted as due to the strong decrease of the ionization rates with an increase of the ionization potential (with increasing vibrational excitation of the molecular ion). Recently, the *S*-matrix overlap model has been reused [11] to investigate the data obtained by Urbain *et al.* [6] in the hydrogen molecule. We note also that, earlier, these experimental data have been analyzed using a modified Keldysh-type tunnel theory of photoionization of molecules, with and without the overlap approximation [12].

In this paper we present the recently proposed (Ref. [4], Sec. 6.4) intense-field many-body *S*-matrix theory (IM*S*T) of IVI of molecules, in which the ionization of the target molecule is accompanied simultaneously by vibrational excitations of the molecular ion. The basic idea of the IM*S*T for the IVI process is a generalization of the "adiabatic nuclei" (in contrast to the "frozen nuclei") theory of vibrational transition by electron impact, originally developed a long time ago [13]. The IM*S*T of IVI is neither restricted to the intensity regime of tunneling or static-field ionization nor does it make an *a priori* use of the overlap approximation. To test the theory and also to be able to assess the related models, we

apply our theory to the case of H_2 and compare its predictions with the experimental data obtained by Urbain *et al.* [6], and discuss the results.

II. *S*-MATRIX THEORY OF INELASTIC VIBRONIC IONIZATION OF MOLECULES

The intense-field many-body *S*-matrix theory [14] provides an *ab initio* approach to analyze the dynamics of atoms and molecules in an intense laser field. In the past it has been successfully applied to the single, double, and multiple ionization of atoms as well as to the ionization of diatomic and polyatomic molecules (for a recent review see Ref. [4]). The theory provides a systematic approximation scheme for obtaining the transition amplitudes between the asymptotic initial and the final states defining the process by taking into account the appropriate partitions in the initial, the final and the intermediate states of the total Hamiltonian of the many-body electronic system interacting with strong laser fields.

The lowest order amplitude of the IM*S*T for the inelastic vibronic ionization of molecules is in fact given by the transition matrix element of the laser interaction operator between the unperturbed initial state of the system (which is a product state of the given vibrational level in the ground electronic state of the neutral molecule) and the final state of the system, that is given by the direct product of the Volkov state of the free electron in the laser field and the final vibrational level of the ground electronic state of the molecular ion (Ref. [4], Sec. 6.4). It corresponds to a direct generalization of the well-known Keldysh-Faisal-Reiss (KFR) amplitude [15] for ionization in intense fields. In this work we assume the Born-Oppenheimer approximation and write the wave function of the neutral molecule in the νth vibrational level of the initial electronic orbital Φ_i (within the single-active-electron ansatz) as

$$\Phi_\nu^{(i)} = \Phi_i(\boldsymbol{r};\mathbf{R}_1,\mathbf{R}_2)\chi_\nu(R-R_e)\exp(-iE_\nu^{(i)}t), \tag{1}$$

where χ_ν is the vibrational wave function, $\mathbf{R}_2-\mathbf{R}_1=\mathbf{R}$, and R_e is the equilibrium distance of the neutral molecule. The final state is given by

$$\Phi_{\nu'}^{(f)} = \chi'_{\nu'}(R-R'_e)\exp(-iE_{\nu'}^{(f)}t)\Phi_{\text{Volkov}}(\boldsymbol{r},t) \tag{2}$$

with the vibrational wave function of the final state $\chi'_{\nu'}$, the Volkov wave function Φ_{Volkov}, and the equilibrium distance R'_e of the molecular ion. The orientation $\hat{\mathbf{R}}$ of the molecule is assumed to be fixed during the ionization process. It is convenient to express the electronic orbitals as linear combinations of atomic orbitals

$$\Phi(\boldsymbol{r};\mathbf{R}_1,\mathbf{R}_2) = \sum_{n=1}^{2}\sum_j b_{n,j}(R)\phi_{n,j}(\boldsymbol{r};\mathbf{R}_n). \tag{3}$$

For the actual computations these wave functions have been obtained using the quantum chemical GAMESS code [16].

According to Eq. (28) of Ref. [4] the first order amplitude for the transition from the initial state in the neutral molecule with vibrational quantum number ν to the vibrational state labeled ν' of the molecular ion, in the general case of an elliptically polarized field, can be written as

$$\begin{aligned} S_{fi}^{(1)}(t_f,t_i) = &-i\sum_{N=-\infty}^{\infty}\int_{t_i}^{t_f}dt_1\exp\left[i\left(\frac{k^2}{2}+U_p+E_T-N\omega\right)t_1\right] \\ &\times(U_p-N\omega)J_N(a,b,\chi)\langle\chi'_{\nu'}(R-R'_e)| \\ &\times\langle\boldsymbol{k}|\Phi_i(\boldsymbol{r};\mathbf{R}_1,\mathbf{R}_2)\rangle|\chi_\nu(R-R_e)\rangle, \end{aligned} \tag{4}$$

where $E_T=E_{\nu'}^{(f)}-E_\nu^{(i)}$ is the IVI transition energy. The inner brackets of the matrix element denote integration over the spatial coordinates of the electron, while the outer brackets represent an integration over the internuclear distance R. $J_N(a,b,\chi)$ are generalized Bessel functions of three arguments (e.g., Ref. [17])

$$J_N(a,b,\chi) = \sum_{m=-\infty}^{\infty} J_{N+2m}(a)J_m(b)\exp[i(N+2m)\chi], \tag{5}$$

where

$$a = \alpha_0\sqrt{\left(\boldsymbol{\epsilon}_1\cdot\boldsymbol{k}_N\cos\frac{\xi}{2}\right)^2+\left(\boldsymbol{\epsilon}_2\cdot\boldsymbol{k}_N\sin\frac{\xi}{2}\right)^2}, \tag{6}$$

$$b = \frac{U_p}{2\omega}\cos\xi, \tag{7}$$

$$\chi = \arctan\left[\tan(\phi_{k,\epsilon})\tan\left(\frac{\xi}{2}\right)\right] \tag{8}$$

which reduces to

$$J_N(a,b) = \sum_{-\infty}^{\infty} J_{N+2m}(\boldsymbol{\alpha}_0\cdot\boldsymbol{k}_N)J_m\left(\frac{U_p}{2\omega}\right) \tag{9}$$

for linear polarization ($\xi=0$) and

$$J_N(a) = J_N\left(\frac{\alpha_0}{\sqrt{2}}k_N\sin\theta_{k,\epsilon}\right)\exp[iN\phi_{k,\epsilon}] \tag{10}$$

for circular polarization ($\xi=\pi/2$), where $\theta_{k,\epsilon}$ and $\phi_{k,\epsilon}$ are the polar angle and azimuth of $\boldsymbol{k}_N$ in a coordinate system where $\boldsymbol{\epsilon}_1$ and $\boldsymbol{\epsilon}_2$ lie in the x-y plane. $U_p=I/4\omega^2$ and $\alpha_0=\sqrt{I}/\omega^2$ are quiver energy and amplitude of the electron in the laser field of intensity I and frequency ω.

The asymptotic time integral turns the time-dependent phase of Eq. (4) into the condition of conservation of energy

$$\begin{aligned} S_{fi}^{(1)} = &-2\pi i\sum_{N=-\infty}^{\infty}\delta\left(\frac{k^2}{2}+U_p+E_T-N\omega\right)(U_p-N\omega)J_N(a,b,\chi) \\ &\times\langle\chi'_{\nu'}(R-R'_e)|\langle\boldsymbol{k}|\Phi_i(\boldsymbol{r};\mathbf{R}_1,\mathbf{R}_2)\rangle|\chi_\nu(R-R_e)\rangle. \end{aligned} \tag{11}$$

Taking the absolute square of this amplitude (by using Eq. (43) of Ref. [4]), the differential rate of transition from the vibronic state of the neutral molecule with vibrational quantum number ν to the vibrational state labeled ν' of the molecular ion by the absorption of N photons from a elliptically polarized field can be written as

$$\frac{dW_{\nu',\nu}^{(f,i)}}{d\hat{\boldsymbol{k}}_N}(I) = 2\pi C^2 N_e k_N (N\omega - U_p)^2 J_N^2(a,b,\chi) \times \left| \sum_{n=1}^{2} \sum_j \langle \chi'_{\nu'}(R-R'_e)|b_{n,j}(R) \times \exp\left(-i\boldsymbol{k}_N \cdot \hat{\mathbf{R}}_n \frac{\mu R}{m_n}\right) |\chi_\nu(R-R_e)\rangle \tilde{\phi}_{n,j}(\boldsymbol{k}_N) \right|^2 \tag{12}$$

in the center of mass frame of the molecule, where the vector $(\mu R_e/m_n)\hat{\mathbf{R}}_n$ points to the equilibrium position of the nth nucleus in the initial electronic state and μ denotes the reduced mass of the molecular system. $\tilde{\phi}_{n,j}(\boldsymbol{k}_N)$ is the Fourier transform of the atomic orbital $\phi_{n,j}$, with $k_N = k_N(\nu',\nu) = \sqrt{2[N\omega - U_p - (E_{\nu'}^{(f)} - E_\nu^{(i)})]}$. N_e denotes the number of equivalent electrons (neglecting spin) in the initial molecular orbital and $C^2 = (2k_T E_T/F)^{2Z/k_T}$ is a Coulomb correction factor with $E_T \equiv k_T^2/2$ [10]. F is the field strength and Z is the charge of the molecular ion in the final state.

To investigate the dependence of the IVI distributions on the choice of the vibrational wave functions, we have used both the well-known harmonic oscillator wave functions (e.g., Ref. [18], Sec. 13) as well as the Morse wave functions for the initial and final vibrational states. The latter are defined as

$$\chi_\nu(x) = \sqrt{\frac{\alpha q_\nu \nu!}{\Gamma(2a-\nu)}} \exp\left[-\frac{y(x)}{2}\right] y(x)^{q_\nu/2} L_\nu^{q_\nu}[y(x)], \tag{13}$$

where the parameters

$$y(x) = 2ae^{-\alpha x} \quad \text{and} \quad x = R - R_e, \tag{14}$$

$$q_\nu = 2a - 1 - 2\nu, \tag{15}$$

$$\alpha = \omega_e \sqrt{\frac{\mu}{2D_e}}, \tag{16}$$

$$a = \frac{2D_e}{\omega_e} \tag{17}$$

are different for the initial and final state. D_e is the energy of dissociation from the minimum of the potential energy curve and ω_e is the vibrational frequency.

We note that the orientation of the molecule in space is determined in Eq. (12) via the unit vectors $\hat{\mathbf{R}}_n = \pm\hat{\mathbf{R}}$. For a diatomic molecule, the orientations in the body-fixed frame (with the molecular axis chosen along the polar axis) of an ensemble of molecules, can be taken into account by averaging over their distribution in the space-fixed laboratory frame. In the theoretical results presented below, we have in general assumed a random distribution of the molecular axes and carried out the orientation averaging, unless otherwise stated explicitly.

The *total* IVI rate of the vibronic transition from a vibrational level ν of the electronic state i of the molecule into the level ν' of the electronic state f of the molecular ion, is given by the integration of Eq. (12) over the ejection angles $\hat{\boldsymbol{k}}_N$ of the photoelectron and the summation over the number of photons N absorbed from the field

$$\Gamma_{\nu',\nu}^{(f,i)}(I) = \sum_{N=N_0}^{\infty} \int d\hat{\boldsymbol{k}}_N \frac{dW_{\nu',\nu}^{(f,i)}}{d\hat{\boldsymbol{k}}_N}(I), \tag{18}$$

where N_0 is the minimum number of photons needed to be absorbed to allow the transition of interest, or $N_0 = \lfloor (E_T + U_p)/\omega \rfloor_{\text{int.}} + 1$. The above formula for the total rate, (18) is valid both in the corresponding "multiphoton" ($\gamma = \sqrt{E_T/2U_p} \gg 1$) and in the "tunnel" ($\gamma \ll 1$) regimes of ionization. We point out that in the tunneling limit Eq. (18) can be evaluated also approximately by, first, using the integral representation of the generalized Bessel function and evaluating it by the usual stationary phase method, and next by replacing the sum over N by an integral over $1/\omega d(N\omega)$ (see, e.g., Ref. [19] or [4]). Thus, it is clear that the present *S*-matrix formalism predicts that even in the tunneling limit, it is the eigenenergy difference between the asymptotic initial and final vibronic states, which is the *transition* energy E_T defined above, rather than the difference with respect to the potential energy curves, which controls the IVI process.

III. RESULTS AND DISCUSSION

In this section we calculate the IVI distributions for H_2 using the lowest order IM*S*T presented above, present the results of the calculations, and compare them with the experimental data of Urbain *et al.* [6]. Next we investigate the origin of the observed shift of the distributions toward the lower vibrational states (compared to the Frank-Condon distribution) as well as the peak-reversal and channel closing phenomena, and discuss the location of the maximum of the distributions. Then we study the role of the alignment of the molecular axis, parallel or perpendicular, to the linear polarization direction of the laser, and consider the effect of circular polarization on the IVI distribution. Using the result of the present "adiabatic nuclei" theory we also assess the "frozen nuclei" overlap approximation, and consider the influence of the choice of the vibrational wave functions. Finally, we present the IVI distributions from the two isotopic variants of H_2 (HD and D_2) and predict an isotopic-shift effect in the IVI process.

It should be noted that in order to compare the theory with the experiment one needs to consider the fact that the experimental data for IVI are obtained (as usual, on a relative scale) as ion population or *yields* generated in the focus of a pulsed laser beam. The latter provides an initial ensemble of neutral target molecules that interact with the laser field during a time interval of the order of the pulse duration, and within a spatial volume of the order of the focal volume. The IVI yield distributions, therefore, are constructed below by substituting the basic theoretical rates of the IVI transitions (of a single molecule) in the rate equations that govern the relative populations of interest. The normalized yield distributions are then obtained, at a given point in the laser focus,

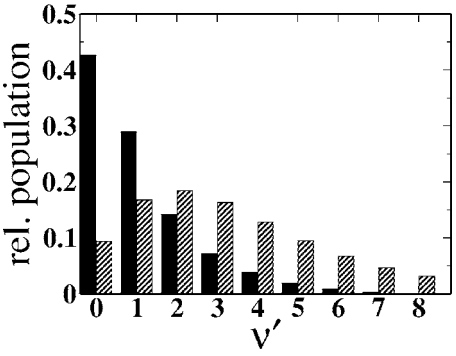

FIG. 1. Comparison of the present calculations of the IVI yield distribution (normalized to the total ion yield from the vibrational channels) of the different vibrational levels of H_2^+ (solid bars) and the corresponding Franck-Condon distribution (hatched bars). Laser parameters: $\lambda=800$ nm, $I_0=3\times10^{13}$ W/cm^2, and $\tau=45$ fs.

by integrating the rate equations over the pulse time profile and adding the contributions from all the points within the focus (e.g. Ref. [20]).

The rate equations for the normalized populations in the final vibrational channels are given by [9]

$$\frac{dN_{\nu'}^{(f)}(t)}{dt}=\Gamma_{\nu',0}^{(f,X)}(I(\boldsymbol{r},t))\left(1-\sum_{\nu'}N_{\nu'}^{(f)}(t)\right), \tag{19}$$

where we have assumed that the target molecule is initially prepared in the lowest vibrational level ($\nu=0$) of its electronic ground state ($i=X$). Furthermore we restrict our analysis to one specific final electronic state, namely, the ground state of the molecular ion; here we do not consider contributions from ionization to any higher charge states [21] and/or possible fragments. In actual computations, we have solved

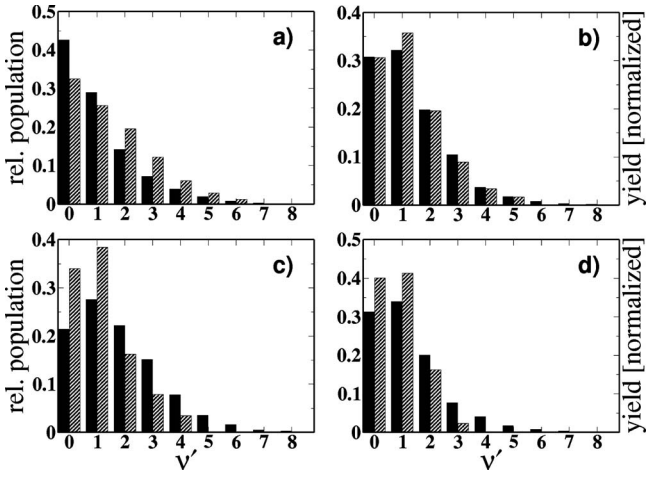

FIG. 2. Comparison of the normalized populations (branching ratios) of the vibrational levels in H_2^+ (solid bars) with the normalized experimental yields taken from Ref. [6] (hatched bars). Laser parameters are (a)–(c) $\lambda=800$ nm, $\tau=45$ fs at $I_0=3\times10^{13}$ W/cm^2 [panel (a)], $I_0=4.8\times10^{13}$ W/cm^2 [panel (b)] and $I_0=1.5\times10^{14}$ W/cm^2 [panel (c)]; (d) $\lambda=1064$ nm, $\tau=6$ ns at $I_0=10^{14}$ W/cm^2.

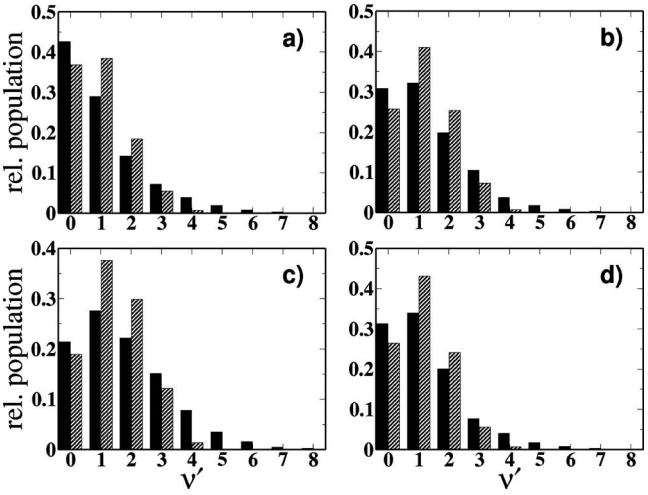

FIG. 3. Effect of the choice of vibrational wave functions on the predicted populations in the molecular H_2^+ ion. Shown is a comparison between the results obtained with Morse (solid bars) wave functions and harmonic oscillator wave functions (hatched bars). Laser parameters are the same as in Fig. 2.

the rate equations, assuming a typical Gaussian temporal laser pulse profile with an (experimentally given) pulse length τ centered around $t=0$; the results are then integrated over the spatial intensity distribution of a Gaussian TEM_{00} mode, characterized by the (experimentally given) peak pulse intensity I_0, the beam waist, and the Rayleigh length of the beam.

A. Results for H_2: Comparison with experimental data

In Fig. 1 we present the result of our calculations (solid bars) for the IVI distribution of population in different vibrational levels of the H_2^+ ion, for the laser wavelength $\lambda=800$ nm, peak intensity $I_0=3\times10^{13}$ W/cm^2, and pulse length $\tau=45$ fs. The orientations of the internuclear axis for the ensemble of molecules has been assumed to be random

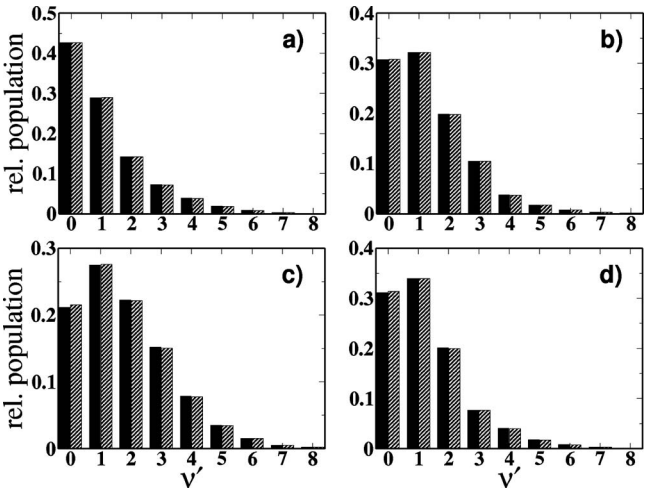

FIG. 4. Comparison of the IVI populations for the alignment of the internuclear axis parallel (solid bars) and perpendicular (hatched bars) to the laser polarization direction. Laser parameters are the same as in Fig. 2.

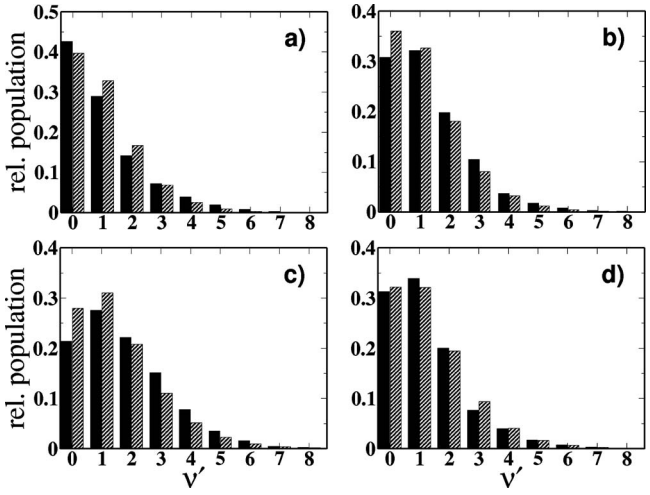

FIG. 5. Comparison of the IVI populations for linear (solid bars) vs circular polarization (hatched bars) of the laser light. Laser parameters are the same as in Fig. 2.

and the averaging over the orientations was carried out. For the sake of comparison we also show in the figure the Franck-Condon overlap distribution for the present case [5] (hatched bars).

A glance at the figure reveals a strong difference between the calculated IVI distribution and the Franck-Condon overlap distribution. While the present result shows a maximum at $\nu'=0$ followed by a continuous decrease toward the higher levels, the Franck-Condon distribution is peaked at $\nu'=2$ and then decreases only slowly. As a consequence, the FC distribution strongly underestimates the populations in the two lowest vibrational levels, and systematically overestimates those from the third level onwards. This is similar to a strong shift toward the lower excitation levels as predicted theoretically earlier [6–9] and observed in the experiment [6] subsequently.

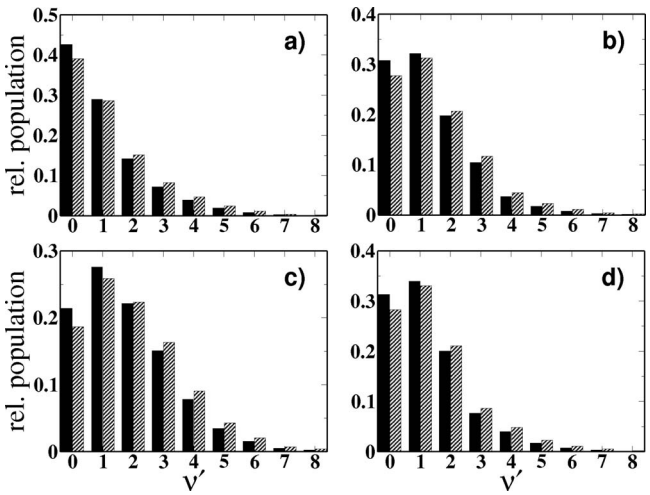

FIG. 6. Comparison of the vibrational populations in the molecular H_2^+ ion as obtained from *S*-matrix calculations with fully *R*-dependent molecular orbitals (solid bars) and with fixed molecular orbital coefficients (hatched bars). Laser parameters are the same as in Ref. 2.

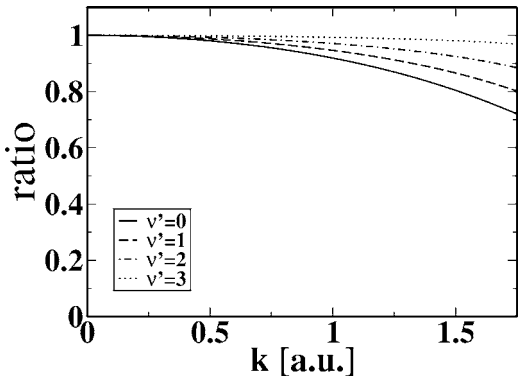

FIG. 7. Variation of the ratio $|t_{\nu',0}(\boldsymbol{k})|^2$ to $|t^{(\mathrm{FC})}_{\nu',0}(\boldsymbol{k})|^2$ as a function of $\boldsymbol{k}$ for different ν' (see legend).

We compare in Fig. 2 the results of the present theory (solid bars) with the experimental data of Urbain *et al.* (hatched bars [6]) at two different wavelengths [(a)–(c): 800 nm, (d): 1064 nm] and four different peak laser intensities (a) $I_0=3\times10^{13}$ W/cm^2, (b) $I_0=4.8\times10^{13}$ W/cm^2, (c) $I_0=1.5\times10^{14}$ W/cm^2, and (d) $I_0=10^{14}$ W/cm^2. A shift toward the lowest vibrational states can be seen clearly to be present in all the cases in the figure.

We observe that although the calculated individual heights are not quite the same, the major characteristics of the theoretical results, including the monotonic decrease of the heights with increasing vibrational excitation in case (a), and the occurrence of a peak reversal in the cases (b), (c), and (d) are fully consistent with the experimental data. More specifically, the theory correctly reproduces the position of the maximum in every distribution (a)–(d), namely, at 800 nm and at the lowest intensity [Fig. 2(a)], it occurs at $\nu'=0$, while in all the other cases the maximum is located at $\nu'=1$, both in the experimental data as well as in the theoretical results. The dominant population of the vibronic

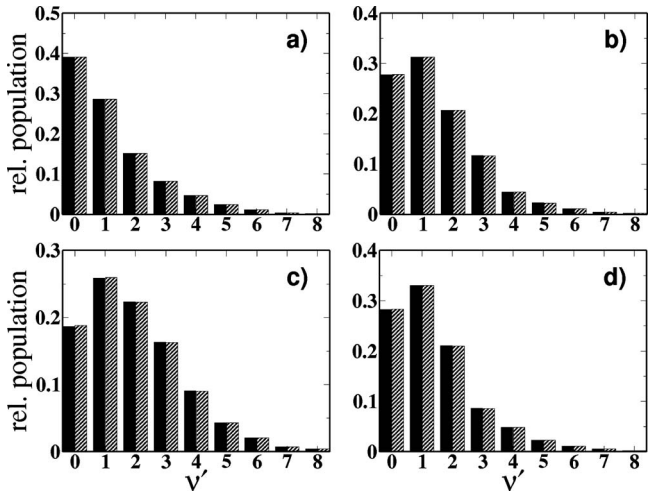

FIG. 8. Comparison of the results (solid bars) of calculations in which the molecular orbital coefficients are fixed at $R=R_e$ (keeping the R dependence of the phase) to those in which the overlap approximation has been assumed (hatched bars). Laser parameters are the same as in Fig. 2.

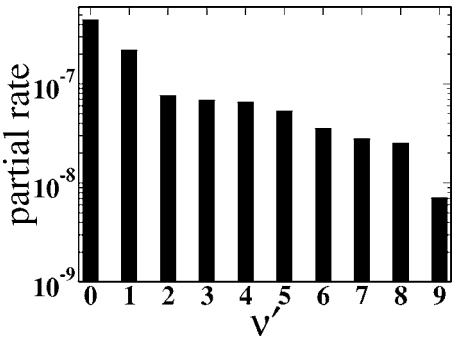

FIG. 9. Variation of the electronic part of the transition rate to $H_2^+(\nu')$ at a peak intensity of $I_0=4.8\times10^{13}$ W/cm^2 for the linear polarized 800 nm case. Note that there are two channel closings at $\nu'=2$ and $\nu'=9$ at this particular intensity.

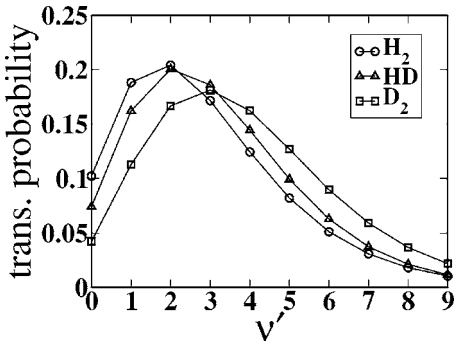

FIG. 11. Calculated Franck-Condon distributions for H_2^+, HD^+, and D_2^+ after direct transition out of the ground state of the respective molecule.

ground state occurs in the calculations in the interval of intensity between 2.5×10^{13} W/cm^2 and 4.1×10^{13} W/cm^2 for 800 nm.

We point out that the remaining difference between the experimental and the calculated yields might be due to two reasons. First, there is an uncertainty of about 20% in the measurement of the peak intensity [6], and we have noted in the calculations that the actual heights are sensitive to the peak intensity of the laser. Second, a possible effect of fragmentation or dissociation of the hydrogen molecular ion is not taken into account in the computations. In fact, Urbain *et al.* [6] have pointed out that depending on the orientation of the molecular ion and the laser intensity, a possible dissociation of the ion into a proton and a hydrogen atom may occur from the higher vibrational states of the ion. This could lead to a depletion of the higher vibrational levels in the experiment and might also be responsible for the overestimations by the present calculations [see Figs. 2(c) and 2(d)] which neglect a possible fragmentation or dissociation induced effect.

Before we proceed further let us point out that the results of the calculated distributions depend strongly on the choice of the vibrational wave functions. This becomes obvious from Fig. 3, where we show a comparison between the IVI distributions obtained with the Morse wave functions (solid bars) and with the simple harmonic oscillator wave functions (hatched bars). The results from the calculations with the harmonic oscillator wave functions clearly show a considerably weaker shift toward lower vibrational states than those obtained from the Morse wave functions. This is not only a quantitative difference but also can lead to a qualitative change. For example, the shift of the position of the distribution maximum from $\nu'=1$ to $\nu'=0$ at the lowest field intensity [see Fig. 3(a)] is not reproduced by the simple harmonic oscillator wave functions [22].

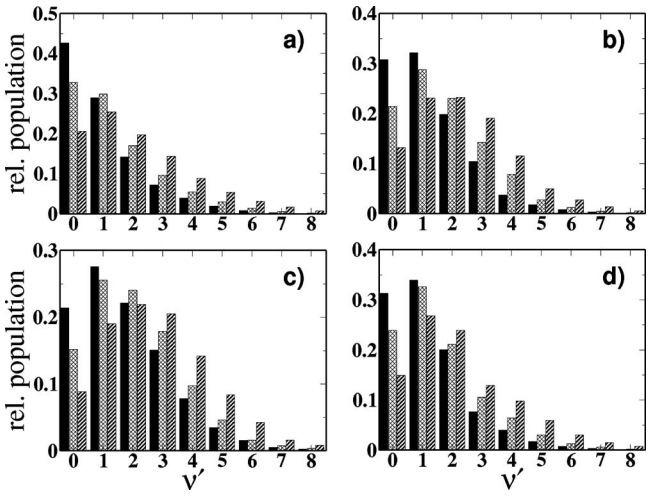

FIG. 10. Normalized populations of the vibrational states in H_2^+ (solid bars), HD^+ (cross hatched bars), and D_2^+ (hatched bars) for IVI of H_2, HD, and D_2, from their respective ground states. Laser parameters are the same as in Fig. 2.

B. Alignment and polarization effects

It has been shown recently (e.g., Refs. [20,23]) that for diatomic molecules both the total ionization rates and the photoelectron angular distributions depend on the orientation of the internuclear axis. In contrast, we have found in the course of the present calculations (and in agreement with results from the static field theory [6]) that the effect of the alignment of the molecule is rather small or negligible for the IVI populations in the vibrational levels of the hydrogen molecular ion (at least as long as the fragmentation effect is considered to be negligible). This is exemplified in Fig. 4, where we compare the results for the alignment of the internuclear axis parallel (solid bars) or perpendicular (hatched bars) to the direction of (linear) polarization of the laser. It can be seen that the results are hardly different in the two cases.

We have further investigated the effect of the choice of the laser polarization on the IVI distributions. In Fig. 5 we show the calculated IVI yields for the circular polarization of the field, at the same intensities and frequencies of the laser as in the linear polarization case Fig. 2. Interestingly, for the circular polarization case we observe the dominant population to be in the vibronic ground state $\nu'=0$, not only for a limited interval of intensities, but increasingly also for all intensities below a certain threshold intensity $I_0=8.2\times10^{13}$ W/cm^2 for 800 nm or $I_0=1.04\times10^{14}$ W/cm^2 for 1064 nm. As a result, while a channel closing effect apparently accounts for the peak reversals in the case of linear

TABLE I. Molecular constants [24–26].

	R_e (Å)	D_0 (eV)	ω_e (cm^{-1})	$\omega_e x_e$ (cm^{-1})	μ_A (a.m.u.)[a]	I_p (eV)
$H_2(X\,^1\Sigma_g^+)$	0.741	4.478	4401.21	121.33	0.5076	15.42593
$H_2^+(X\,^2\Sigma_g^+)$	1.052	2.65	2322.0	66.2	0.5076	
$HD(X\,^1\Sigma_g^+)$	0.74142	4.513789	3813.1	91.65	0.672	15.44465
$HD^+(X\,^2\Sigma_g^+)$	1.057	2.667682	1913.1	40.72[b]	0.672	
$D_2(X\,^1\Sigma_g^+)$	0.74152	4.556256	3115.5	61.82	1.007	15.46658
$D_2^+(X\,^2\Sigma_g^+)$	1.0559	2.691919	1577.3	27.64[b]	1.007	

[a] $m_e = 5.4858 \times 10^{-4}$ a.m.u. [26].
[b] Calculated values.

polarization [11], in the circular polarization case the vibronic ground state of the molecular ion is favored for all intensities, with out a peak reversal, below the abovementioned thresholds.

C. Analysis and discussion

In order to analyze the origin of the stronger population of lower vibrational levels than in the Franck-Condon distributions, we have first investigated whether the overlap approximation is violated in this process. In the expression for the differential IVI rate [Eq. (12)], the electronic and the vibrational matrix elements are coupled by two factors that depend on the internuclear distance R, namely, the molecular orbital coefficients $b_{n,j}(R)$ and the dynamical phase appearing in the exponential function. In order to analyze the influence of both these factors, we first treated the MO coefficients as constants evaluated at the molecular equilibrium separation, while the dynamical phase was allowed to vary with R. In this approximation the IVI rate is given by the formula

$$\frac{dW_{\nu',\nu}^{(f,i)}}{d\hat{\boldsymbol{k}}_N}(I) \approx 2\pi C^2 N_e k_N (N\omega - U_p)^2 J_N^2(a,b,\chi) \times \left| \sum_{n=1}^{2} \sum_j b_{n,j}(R_e)\tilde{\phi}_{n,j}(\boldsymbol{k}_N)\langle \chi'_{\nu'}(R-R'_e)| \times \exp\left(-i\boldsymbol{k}_N \cdot \hat{\mathbf{R}}_n \frac{\mu R}{m_n}\right)|\chi_\nu(R-R_e)\rangle \right|^2. \quad (20)$$

In Fig. 6 we compare results obtained within this assumption from the above equation to those from the full calculations, Eq. (12). It can be seen that in all cases considered, the shift toward the lowest vibrational levels is somewhat smaller in the calculations with the "frozen nuclei" MO coefficients, however, the distinct departure from the Franck-Condon distribution, the shift toward lower vibrational states and the reversal of the peak position are still present.

To analyze the effect of the variation of the phase factor with the internuclear distance R, we note that for ionization of the hydrogen molecule from its ground state Eq. (20) can be rewritten as

$$\frac{dW_{\nu',\nu}^{(f,i)}(I)}{d\hat{\boldsymbol{k}}_N} = 2\pi C^2 N_e k_N (N\omega - U_p)^2 J_N^2(a,b,\chi) |\tilde{\phi}(\boldsymbol{k}_N)|^2 \times \underbrace{4\langle \chi'_{\nu'}(R-R'_e)|\cos\{\arg[\tilde{\phi}(\boldsymbol{k}_N)] + \boldsymbol{k}_N \cdot \mathbf{R}/2\}|\chi_\nu(R-R_e)\rangle^2}_{|t_{\nu',\nu}(\boldsymbol{k}_N)|^2}, \quad (21)$$

where

$$\tilde{\phi}(\boldsymbol{k}_N) = \sum_j b_j(R_e)\langle \boldsymbol{k}_N|\phi_j(\boldsymbol{r};-\mathbf{R}_e/2)\rangle \quad (22)$$

is the Fourier transform of the part of the molecular wave function localized at the nucleus at $\mathbf{R}_1 = -\mathbf{R}_e/2$ and $\hat{\mathbf{R}}_e$ points along the molecular axis away from that nucleus.

In the overlap approximation it is assumed that the electronic $\boldsymbol{k}$ dependence decouples in the matrix element between the vibrational wave functions, and reduces the latter to

$$|t_{\nu',\nu}^{(\mathrm{FC})}(\boldsymbol{k})|^2 = 4\cos^2\{\arg[\tilde{\phi}(\boldsymbol{k}_N)] + \boldsymbol{k}_N \cdot \mathbf{R}_e/2\} \times \langle \chi'_{\nu'}(R-R'_e)|\chi_\nu(R-R_e)^2. \quad (23)$$

In Fig. 7 we present the ratio of the partial matrix element $|t_{\nu',0}(\boldsymbol{k})|^2$ to $|t_{\nu',0}^{(\mathrm{FC})}(\boldsymbol{k})|^2$, averaged over all angles of electron ejection $\hat{\boldsymbol{k}}$ as a function of k and for different vibrational numbers ν'. As can be seen from the figure, the ratio is close to 1 for small values k. This may be simply understood from the leading constant term of the Taylor expansion of the phase factor. Thus, since the rate of laser induced ionization

is dominated by the emission of slow electrons, the conditions for the overlap approximation should be well fulfilled in the present case (see Fig. 7). It may deviate, however, should higher kinetic energies be observed, e.g., in the differential probability distributions.

To check our expectation, we did test calculations where we have replaced $|t_{0,\nu'}(\boldsymbol{k})|^2$ by $|t^{(\mathrm{FC})}_{0,\nu'}(\boldsymbol{k})|^2$ in Eq. (20). Figure 8 shows the results of these calculations. As can be seen from the figure the results (hatched bars) are nearly identical. Together with Fig. 6 this shows, that the overlap approximation, which has been assumed before in *S*-matrix calculations in an *ad hoc* way [9,11], is a qualitatively good approximation at the present field parameters.

Therefore, the main cause of the shift in the distribution of the IVI probability to move away from the Franck-Condon distribution to lower vibrational quantum numbers, lies in the nonlinear dependence of the ionization rate on the transition energy $E_T=E^{(f)}_{\nu'}-E^{(i)}_{\nu}$. As has been noted before [9,11] and as can be seen from Fig. 9, the increase of the transition energy results in a strong decrease of the electronic transition rate itself. A Franck-Condon-like distribution of IVI would have resulted only if ionization rates for different inelastic vibrational channels would have been approximately a constant. This is clearly not the case. Rather, due to the strong decrease of the ionization rates with increasing inelasticity, the population of the higher vibrational states in IVI is *suppressed* below the Franck-Condon distribution.

D. Application to HD and D_2

Next, we have applied the present theory to investigate a possible presence of an isotopic effect in the IVI processes. To this end, we have calculated the IVI distributions from two isotopes of hydrogen molecule HD and D_2. We may note parenthetically that while for the neutral species the molecular constants needed for the Morse wave functions are available in literature [24], for the molecular ions we calculated the anharmonicity parameter $\omega_e x_e=\omega_e^2/(4D_e)$, which determines the eigenenergies of the vibrational states, from the experimental values [25] of the energy $D_0=D_e-\omega_e/2$. The relevant constants are given in Table I.

In Fig. 10 we present the results for the calculated IVI distributions from the ground vibronic states of the isotopes. The computations have been carried out at the same laser parameters as for the hydrogen molecule (see Fig. 2). A small but clear *isotopic shift* of the IVI distributions of the *heavier* isotopes of H_2 toward the higher vibrational levels is predicted. We may note that, as the decrease of the electronic part of the transition rate as a function of the inelastic vibrational excitations is rather similar for the three molecules, the differences in the distributions are mainly due to the different behavior of the vibrational part. This is also seen from the Franck-Condon factors for the molecules, as presented in Fig. 11, that are obtained from the overlap integrals of the Morse wave functions, as used for the calculations shown in Fig. 10.

IV. CONCLUSIONS

We have presented the lowest-order intense-field many-body *S*-matrix theory of IVI (inelastic vibronic ionization) of diatomic molecules, in which the ionization of a molecule in an intense laser field is accompanied simultaneously by vibrational excitations of the molecular ion, and derived explicit expressions for the corresponding transition rates. The theory is applied to investigate the IVI of hydrogen molecule. The main characteristics of the experimentally observed distributions are found to be reproduced well by the theory. In particular, the experimentally observed shift of the distributions toward the lowest vibrational levels (as compared to a Franck-Condon distribution) are found to be due to the strong nonlinear dependence of the transition rates on the transition energy of the process. In the case of linear polarization the so-called channel closing effect is observed but for the circular polarization case this effect does not seem to play any role in determining the maximum of the IVI distributions. The role of the "frozen nuclei" overlap approximation is investigated using the present "adiabatic nuclei" *S*-matrix theory. It is found that the quantitative effect of the "frozen nuclei" approximation is to shift the population of the vibrational states less toward the lowest quantum numbers, but it does not change the qualitative behavior, for the laser parameters considered. The effect of alignments of the molecular axis is discussed; the difference in the distributions obtained with the molecular axis, along (parallel) or perpendicular to the (linear) polarization axis of the laser, are found to be quite negligible. Finally, the IVI distributions of the isotopes HD and D_2 are determined and an *isotopic shift* of the distributions toward the higher vibrational states, in the case of the heavier isotopes, is predicted.

[1] *Molecules in Laser Fields*, edited by A. D. Bandrauk (Marcel Dekker, New York, 1994).
[2] *Molecules and Clusters in Intense Laser Fields*, edited by J. H. Posthumus (Cambridge University Press, Cambridge, 2001).
[3] J. H. Posthumus, Rep. Prog. Phys. **67**, 623 (2004).
[4] A. Becker and F. H. M. Faisal, J. Phys. B **38**, R1 (2005).
[5] G. H. Dunn, J. Chem. Phys. **44**, 2592 (1966).
[6] X. Urbain, B. Fabre, V. M. Andrianarijaona, J. Jureta, J. H. Posthumus, A. Saenz, E. Baldit, and C. Cornaggia, Phys. Rev. Lett. **92**, 163004 (2004).
[7] A. Saenz, J. Phys. B **33**, 4365 (2000).
[8] A. Saenz, Phys. Rev. A **66**, 063408 (2002).
[9] A. Becker, A. D. Bandrauk, and S. L. Chin, Chem. Phys. Lett. **343**, 345 (2001).
[10] J. Muth-Böhm, A. Becker, and F. H. M. Faisal, Phys. Rev. Lett. **85**, 2280 (2000).
[11] T. K. Kjeldsen and L. B. Madsen, Phys. Rev. Lett. **95**, 073004 (2005).
[12] K. Mishima, K. Nagaya, M. Hayashi, and S. H. Lin, Phys. Rev. A **70**, 063414 (2004).

[13] F. H. M. Faisal and A. Temkin, Phys. Rev. Lett. **28**, 203 (1972).

[14] F. H. M. Faisal and A. Becker, in *Selected Topics on Electron Physics*, edited by D. H. Campbell and H. Kleinpoppen (Plenum, New York, 1996), p. 397.

[15] L. V. Keldysh, Zh. Eksp. Teor. Fiz. **47**, 1945 (1964); [Sov. Phys. JETP **20**, 1307 (1965)]; F. H. M. Faisal, J. Phys. B **6**, L312 (1973); H. R. Reiss, Phys. Rev. A **22**, 1786 (1980).

[16] M. W. Schmidt *et al.*, J. Comput. Chem. **14**, 1347 (1993).

[17] A. Becker, L. Plaja, P. Moreno, M. Nurhuda, and F. H. M. Faisal, Phys. Rev. A **64**, 023408 (2001).

[18] L. I. Schiff, *Quantum Mechanics* (McGraw-Hill, New York, 1968).

[19] A. M. Perelomov, S. V. Popov, and M. V. Terent'ev, Zh. Eksp. Teor. Fiz. **50**, 1393 (1966); [Sov. Phys. JETP **23**, 924 (1966)].

[20] A. Jaroń-Becker, A. Becker, and F. H. M. Faisal, Phys. Rev. A **69**, 023410 (2004).

[21] This might be justified in view of the bonding (gerade) symmetry of the ground state of the H_2, HD, and D_2 molecules, and for the intensity regime below 2×10^{14} W/cm^2, considered in the present calculations.

[22] We noted two misprints in Eqs. (96) and (98) of Ref. [4], Sec. 6.4, which should read

$$b_n = \left(\frac{2\alpha'}{\lambda}\right)^{-2n}\sum_{m=0}^{\lfloor\nu/2\rfloor}\frac{(\alpha'/\alpha)^{2m}}{m!\,(\nu-2m)!\,(n-m)!\,[\nu'-2(n-m)]!},$$

$$I(s,p) = \sqrt{2\pi}\exp\left(-\frac{p^2}{2}\right)\sum_{k=0}^{\lfloor s/2\rfloor}\frac{s!}{(s-2k)!\,k!\,2^k}(ip)^{s-2k}.$$

For the ion $\chi'_{\nu'}(x')$ depends on different parameters $x'=R-R'_e$, and α', which turns the integral over the internuclear coordinate R into an expression similar to those treated in quantum chemical calculations with Gaussian type orbitals. We found, however, that it is more convenient to compute the one dimensional vibrational transition integral by direct numerical quadrature, rather than from the analytical expressions.

[23] A. Jaroń-Becker, A. Becker, and F. H. M. Faisal, J. Phys. B **36**, L375 (2003).

[24] NIST Chemistry WebBook (http://webbook.nist.gov/chemistry), Standard Reference Database Number 69, June 2005 Release.

[25] Y. P. Zhang, C. H. Cheng, J. T. Kim, J. Stanojevic, and E. E. Eyler, Phys. Rev. Lett. **92**, 203003 (2004).

[26] A. A. Radzig and B. M. Smirnov, *Reference Data on Atoms, Molecules and Ions* (Springer, Berlin, 1985).